

## Structure of the Oxygen Point Defect in $\text{SnMo}_6\text{S}_8$ and $\text{PbMo}_6\text{S}_8$

D. G. Hinks, J. D. Jorgensen, and H.-C. Li<sup>(a)</sup>

Materials Science and Technology Division, Argonne National Laboratory, Argonne, Illinois 60439

(Received 27 July 1983)

Rietveld structural refinement of neutron powder diffraction data for Chevrel-phase samples in both the Sn-Mo-S-O and Pb-Mo-S-O systems has led to a model for an oxygen-containing point defect. The oxygen substitutes for the sulfur located in the special position along the  $\bar{3}$  axis and the metal ion is displaced  $\approx 0.8$  Å toward the oxygen impurity, presumably forming a covalent bond. This defect is responsible for the wide variation reported for  $T_c$  and  $c/a$  (hexagonal, lattice-constant ratio).

PACS numbers: 74.70.Dg, 61.70.Ey

The ternary molybdenum chalcogenides  $M_x\text{Mo}_6\text{C}_8$  ( $M$  = metal ion;  $C$  = S, Se, or Te) are a large class of materials showing interesting structural, superconducting, and magnetic behavior.<sup>1-3</sup> Materials containing large metal ions (Pb, Sn, or rare-earth ions) should be stoichiometric at a 1-6-8 composition. However, wide variations of the single-phase composition (or region),  $T_c$ , and structural parameters appear in the literature.<sup>4</sup> This has led many investigators to the belief that intrinsic defects (S or Sn vacancies, Mo interstitials, ...) are formed during the synthesis and that these defects are responsible for the variation in the superconducting properties.<sup>5,6</sup> Recently, we have shown<sup>7</sup> that oxygen can indeed be incorporated into  $\text{SnMo}_6\text{S}_8$  and that the resultant values of  $T_c$  and  $c/a$  (hexagonal, lattice-constant ratio) cover the entire reported range for these parameters.

This Letter reports the structure of the oxygen point defect in  $\text{SnMo}_6\text{S}_8$  and  $\text{PbMo}_6\text{S}_8$ . The structure of the defect has been determined from Rietveld structural refinement of neutron powder diffraction data and gives some insight into the possible mechanisms for depression of  $T_c$ .

Samples were synthesized as reported previously for the Sn-Mo-S-O system.<sup>7</sup> For the Pb system an apparent single phase was also found at a composition  $M_1\text{Mo}_{6.05+x}\text{S}_8\text{O}_x$ . Figure 1 shows the variation in  $T_c$  and  $c/a$  with added oxygen in each system. In each system there is a rapid decrease in  $T_c$  and a reduction in the  $c/a$  ratio (with  $a \approx \text{const}$ ,  $c$  decreasing). Indeed, quantitatively, both systems respond similarly to added oxygen;  $dT_c/dx$ ,  $d(c/a)/dx$ , and the saturation value are nearly the same. This suggests that the same defect is formed in each system.

Neutron powder diffraction measurements were performed on the samples with starting compositions given in Table I with the special environ-

ment powder diffractometer (SEPD) at Argonne's intense pulsed neutron source. The SEPD is a time-of-flight diffractometer on a 14-m incident flight path and has large-area, time-focused detector banks at  $2\theta = 145^\circ$ ,  $90^\circ$ ,  $57^\circ$ , and  $22^\circ$ . The Rietveld structural refinements were done with high-resolution ( $\Delta d/d = 0.35\%$  full width at half maximum) data from the backscattering ( $145^\circ$ ) detectors. In the Rietveld method, a calculated diffraction spectrum is fitted to the raw data with the structural parameters (atom positions, temperature factors, and occupancies) being the variables in the least-squares minimization.<sup>8</sup> This technique allows the maximum amount of information to be obtained from the powder dif-

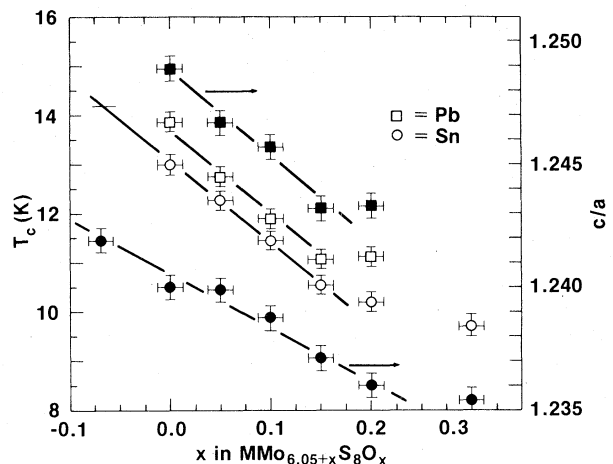


FIG. 1. The variation in  $T_c$  and  $c/a$  with added oxygen ( $x$ ) for the Chevrel phase formed in the quaternary  $M$ -Mo-S-O system (squares, Pb; circles, Sn). Filled and open symbols denote  $c/a$  and  $T_c$ , respectively. The Sn data are from Ref. 7 and show the extrapolation of the  $T_c$ - $x$  line to 14.2 K ( $T_c$  for a "gettered" oxygen-free sample). The displacement of the origin of the  $x$  axis ( $\Delta x \approx -0.7$ ) gives an estimate of the oxygen unintentionally incorporated during synthesis.

TABLE I. Refined site occupancies (with standard deviations in parentheses) for  $\text{SnMo}_6\text{S}_8$  and  $\text{PbMo}_6\text{S}_8$  samples containing oxygen.  $M1$  and  $M2$  are the original and displaced metal sites, respectively.

	$n(M1)$	$n(M2)$	$n(S2)$	$n(O)$
$\text{SnMo}_{6.05}\text{S}_8$	0.96(1)	0.04(1)	1.89(5)	0.11(5)
$\text{SnMo}_{6.15}\text{S}_8\text{O}_{0.10}$	0.92(2)	0.08(2)	1.99(6)	0.01(6)
$\text{SnMo}_{6.25}\text{S}_8\text{O}_{0.20}$	0.82(1)	0.18(1)	1.80(5)	0.20(5)
$\text{PbMo}_{6.20}\text{S}_8\text{O}_{0.15}$	0.88(1)	0.12(1)	1.87(6)	0.12(6)

fraction data. Data collection times were typically 15–20 h for 10-g samples. Although the x-ray diffraction patterns showed no impurity phases, the neutron diffraction patterns did show small Mo peaks.

Initial, unconstrained refinements for the  $\text{SnMo}_{6.05+x}\text{S}_8\text{O}_x$  samples showed that the insertion of oxygen caused the formation of Sn vacancies at a concentration which scaled with added oxygen. However, the overall chemical composition of our single phase did not show a corresponding net loss of Sn. Thus, Fourier mapping techniques were used to search for Sn missing from the original position at the origin. The largest unexplained density in the map was a site along the  $\bar{3}$  axis displaced  $\approx 0.8 \text{ \AA}$  from the origin. Sn located at this site would require an unacceptably short Sn-S bond along the  $\bar{3}$  axis and indicated that in the defected cells one of the axial sulfur atoms is replaced by oxygen. Unconstrained Rietveld refinements which included Sn at both the origin (Sn1) and the displaced site (Sn2) gave total Sn concentrations near unity, thus indicating the correctness of the model. The final refinements were done with the total Sn [ $n(\text{Sn1}) + n(\text{Sn2})$ ] constrained to 1.0 and the total occupancy of the S2 site [ $n(\text{S2}) + n(\text{O})$ ] constrained to 2.0. Mo and S1 occupancies were held at their ideal values of 6. This choice of variable parameters was justified by  $R$ -value ratio-test comparisons with other possible models. The final weighted profile  $R$  values<sup>9</sup> were below 5% ( $\chi^2 < 3.5$ ) for all samples. All temperature factors and atom positions not fixed by symmetry were also refined.

The refined site occupancies for the original and displaced Sn sites and for S and O at the S2 site are given in Table I. Since oxygen at these concentrations represents a small change in scattering density at the S2 site (and there is also some correlation to the S2 Debye-Waller factor which probably includes static effects in the de-

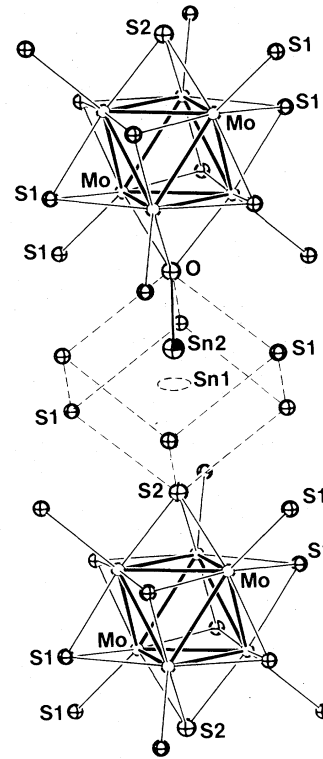


FIG. 2. The structure of the oxygen defect in  $\text{SnMo}_6\text{S}_8$ . The dashed thermal ellipsoid is the normal Sn site (Sn1) at the origin of the unit cell.

fecting structure), the standard deviations for  $n(\text{S2})$  and  $n(\text{O})$  are relatively large. However, the agreement of  $n(\text{O})$  and  $n(\text{Sn2})$ , and, more importantly, the agreement of  $n(\text{Sn2})$ , with the value expected based on starting composition, is a valuable confirmation of the correctness of the structural model. Full structural information from the refinements will appear in a future paper.

This model requires a unit cell composition of  $\text{Sn}_1\text{Mo}_6\text{S}_{8-x}\text{O}_x$ . This is close to the observed single-phase starting composition normalized to  $\text{Mo}_6$ ; i.e.,  $(6/6.25)\text{SnMo}_{6.25}\text{S}_8\text{O}_{0.20} \rightarrow \text{Sn}_{0.96}\text{Mo}_6\text{S}_{7.68}\text{O}_{0.19}$  which is about 4 and 2 at.% deficient in Sn and S, respectively. The presence of unintentionally added oxygen (estimated to be  $\approx 0.07$  from Fig. 1) and the observed occurrence of excess Mo in our samples would both reduce the composition difference between our single-phase and the ideal composition. The remaining impurity phases could easily be below the sensitivity of the measurements used in this study.

The local structure in the region of an oxygen defect is shown in Fig. 2. In the normal  $\text{SnMo}_6\text{S}_8$

TABLE II. Lattice constants and selected atom-atom distances ( $\text{\AA}$ ) for  $\text{SnMo}_{6.05+x}\text{S}_8\text{O}_x$  samples.

	$x=0.0$	$x=0.1$	$x=0.2$
Lattice			
$a$	9.1787(3)	9.1797(4)	9.1768(3)
$c$	11.3770(2)	11.3576(3)	11.3325(3)
$V$ ( $\text{\AA}^3$ )	830.08(8)	828.8(1)	826.48(8)
$\text{Mo}_6\text{S}_8$ cube			
Mo-Mo ( $\Delta$ ) <sup>a</sup>	2.663(2)	2.661(3)	2.656(3)
Mo-Mo ( $\Delta$ - $\Delta$ ) <sup>b</sup>	2.726(2)	2.725(2)	2.725(2)
Mo-Mo (inter)	3.238(2)	3.238(3)	3.239(3)
Mo-S1	2.450(3)	2.451(4)	2.445(4)
Mo-S1	2.464(3)	2.463(3)	2.465(3)
Mo-S1	2.527(4)	2.528(4)	2.531(4)
Mo-S1 (inter)	2.555(3)	2.553(3)	2.551(4)
Mo-S2	2.401(4)	2.399(5)	2.366(4)
S1-S1	3.438(3)	3.436(4)	3.434(4)
S1-S2	3.504(4)	3.505(4)	3.481(4)
Sn site			
Sn1-Sn2	...	0.76(8)	0.83(3)
Sn2-O	...	1.95(8)	1.91(3)

<sup>a</sup>Mo-Mo intracluster distance within a  $\text{Mo}_3$  unit perpendicular to the  $\bar{3}$  axis.

<sup>b</sup>Mo-Mo intracluster distance between two  $\text{Mo}_3$  units perpendicular to the  $\bar{3}$  axis.

structure, Sn is located at the origin, halfway between the two S2 atoms on the  $\bar{3}$  axis and is not strongly bonded to any of its sulfur neighbors. In unit cells where an oxygen atom replaces one of the S2 atoms, the Sn atom moves off the origin and forms a short Sn-O bond. Several atom-atom distances for the three oxygen concentrations studied are listed in Table II. It is clear from these results that the Mo-Mo and Mo-S bond lengths in the  $\text{Mo}_6\text{S}_8$  cluster are not dramatically perturbed by the oxygen defect. Furthermore, the intercluster distances (both Mo-Mo and Mo-S1) remain constant. Locally, the structure collapses toward the oxygen impurity. The Mo-Mo ( $\Delta$ ), Mo-S2, and S1-S2 bonds all shorten indicating the presence of the smaller oxygen atom. In interpreting these results, it should be remembered that the refined S2 position (and to a much lesser extent, all atom positions) is a spatial average of the positions of sulfur and oxygen in the S2 site. Thus, the actual Mo-O bonds are shorter and the Sn-O bond is longer than the refined values indicated in Table II.

A structural refinement for a sample of starting composition  $\text{PbMo}_{6.20}\text{S}_8\text{O}_{0.15}$  confirmed that the same defect structure exists in the Pb Chevrel phase. The refined site occupancies for the

same model are given in Table I. As expected from the larger radius of Pb, the Pb-O bond is longer than the Sn-O bond, 2.01 vs 1.91  $\text{\AA}$ .

The observed Sn-O and Pb-O bond lengths are significantly shorter than those expected for divalent ions in normal (6) coordination ( $\text{Sn}^{+2}\text{-O}^{-2} = 2.45 \text{\AA}$ ,  $\text{Pb}^{+2}\text{-O}^{-2} = 2.59 \text{\AA}$ <sup>9</sup>). This could be due to the low effective coordination of Sn (Pb) (possibly 1) or to a change in the effective charge to  $\text{Sn}^{+4}$  ( $\text{Pb}^{+4}$ ). If the metal ion increased its oxidation state, the rapid decrease in  $T_c$  could be explained as a filling of the Mo  $d$  bands (reducing the density of states at the Fermi energy). An increase in the number of electrons in the  $\text{Mo}_6\text{S}_8$  cluster should be accompanied by a decrease in the Mo-Mo ( $\Delta$ - $\Delta$ ) distance<sup>2</sup>; this decrease is not observed in our structural results (Table II). However, it may be possible for elastic effects to mask the expected contraction. Thus, the charge state of Sn (Pb) should be considered an open question until a suitable local measurement can be performed.

The identification of a specific defect which leads to a depression of  $T_c$  suggests the possibility of investigating the mechanism which suppresses superconductivity. In addition to the charge-transfer effect already discussed, other

band effects as well as phonon effects should be investigated.

We wish to thank G. K. Shenoy, B. Dunlap, and A. Umarji for the many helpful discussions. This work was supported by the U.S. Department of Energy.

---

<sup>(a)</sup>Visiting scientist: Institute of Physics, Chinese Academy of Sciences, Beijing, People's Republic of China.

<sup>1</sup>Ø. Fischer, *J. Appl. Phys.* **16**, 1 (1978).

<sup>2</sup>K. Yvon, in *Current Topics in Materials Science*, edited by E. Kaldis (North-Holland, Amsterdam, 1979), Vol. 3, pp. 53-129.

<sup>3</sup>R. Chevrel and M. Sergent, in *Topics in Current*

*Physics*, edited by Ø. Fischer and M. B. Maple (Springer-Verlag, Berlin, 1982), Vol. 32, pp. 25-86.

<sup>4</sup>R. Flükiger and R. Baillif, in *Topics in Current Physics*, edited by Ø. Fischer and M. B. Maple (Springer-Verlag, Berlin, 1982), Vol. 32, pp. 113-142.

<sup>5</sup>R. Chevrel, C. Russell, and M. Sergent, *J. Less-Common Met.* **72**, 31 (1980).

<sup>6</sup>F. S. Delk, II, and M. J. Sienko, *Inorg. Chem.* **19**, 788 (1980).

<sup>7</sup>D. G. Hinks, J. D. Jorgensen, and H.-C. Li, to be published.

<sup>8</sup>R. B. von Dreele, J. D. Jorgensen, and C. G. Windsor, *J. Appl. Crystallogr.* **15**, 581 (1982). Also H. M.

Rietveld, *J. Appl. Crystallogr.* **2**, 65 (1969).

<sup>9</sup>S. K. Dickinson, Jr., "Ionic, Covalent and Metallic Radii of the Chemical Elements," Air Force Cambridge Research Laboratory Report No. 870-0727, 1970 (unpublished).